15

Recent Developments on Silicon Carbide Thin Films for Piezoresistive Sensors Applications

Mariana Amorim Fraga[1,2], Rodrigo Sávio Pessoa[2,3], Homero Santiago Maciel[2] and Marcos Massi[2]
[1]*Institute for Advanced Studies*
[2]*Plasma and Processes Laboratory, Technological Institute of Aeronautics*
[3] *IP&D, University of Vale do Paraiba*
Brazil

1. Introduction

The increasing demand for microelectromechanical systems (MEMS) as, for example, piezoresistive sensors with capabilities of operating at high temperatures, mainly for automotive, petrochemical and aerospace applications, has stimulated the research of alternative materials to silicon in the fabrication of these devices. It is known that the high temperature operating limit for silicon-based MEMS sensors is about 150ºC (Fraga, 2009).

Silicon carbide (SiC) has shown to be a good alternative to silicon in the development of MEMS sensors for harsh environments due to its excellent electrical characteristics as wide band-gap (3 eV), high breakdown field strength (10 times higher than Si) and low intrinsic carrier concentration which allow stable electronic properties under harsh environments (Cimalla et al., 2007; Wright & Horsfall, 2007; Rajab et al., 2006). In addition, SiC exhibits high elastic modulus at high temperatures which combined with the excellent electronic properties make it very attractive for piezoresistive sensors applications (Kulikovsky et al., 2008).

Silicon carbide can be obtained in bulk or film forms. In recent years, great progress has been made in the field of the growth of SiC bulk. Currently there are 6H-SiC, 4H-SiC and 3C-SiC wafers commercially available. However, these wafers are still very expensive (Hobgood et al., 2004; Camassel & Juillaguet, 2007), so encouraging studies on crystalline and amorphous SiC films deposited on silicon or SOI (Silicon-On-Insulator) substrates using appropriate techniques. The use of SiC films besides being less expensive has another advantage which is the well known processing techniques for silicon micromachining. The challenge is to obtain SiC films with mechanical, electrical and piezoresistive properties as good as the bulk form.

Nowadays, some research groups have studied the synthesis and characterization of SiC films obtained by different techniques namely, plasma enhanced chemical vapour deposition (PECVD), molecular beam epitaxy (MBE), sputtering, among others, aiming MEMS sensors applications (Chaudhuri et al., 2000; Fissel et al., 1995; Rajagopalan et al., 2003; Lattemann et al., 2003).

The purpose of this chapter is to present an overview of the deposition techniques of SiC films, summarizing the deposition conditions that affect the piezoresistive properties of these films, the influence of the temperature on their piezoresistive properties and comparing the performance of piezoresistive sensors based on SiC films with those based in other materials. Moreover, the chapter focus attention is on the development of pressure sensors and accelerometers based on SiC films with suited piezoresistive properties to substitute the silicon in the microfabrication of these sensors so as to extend their endurance under harsh environment.

2. Piezoresistive effect in SiC

2.1 Brief overview

Piezoresistivity is a physical property which has been widely used to convert a mechanical signal into an electrical one, in different device types such as pressure sensors, accelerometers, tactile sensors, strain gauges and flow sensors, among others.

The piezoresistive effect was discovered by Lord Kelvin in 1856. This property is quantified in terms of gauge factor (*GF*), which is defined as the fractional change in the resistance per unit strain (Window, 1992):

$$GF = \frac{\Delta R}{R}\frac{1}{\varepsilon} \tag{1}$$

where R is the nominal electrical resistance and ε the strain. *GF* is a dimensionless number that depends on the crystallographic orientation and is related to the elastic or Young's modulus of the material (E) by the following expression,

$$E = \frac{\sigma}{\varepsilon} \tag{2}$$

where σ is the mechanical stress. A positive *GF* indicates an increase in resistance with stress increases whereas the negative correspond a decrease.

Thus, from eq. (1) and (2), the piezoresistivity can be defined as the fractional change in the resistivity of a material when submitted to a mechanical stress. The change in resistance arises from two effects: the change in the dimension of the resistor and the change in the resistivity of the material itself.

The large piezoresistive effect in silicon and germanium was first observed by Smith in 1954. Since then, it has been noted that the piezoresistive effect in semiconductor materials is highly anisotropic and exhibits a dependence on the dopant type, dopant concentration and crystalline orientation. Furthermore, in 1956 Morin et al. demonstrated the temperature dependence of the piezoresistance of silicon and germanium.

In 1968, Rapatskaya et al. were the first to report the piezoresistive properties of n-type α-SiC (6H-SiC). In the 70's three papers on piezoresistance in SiC were published by Guk: two on the piezoresistive characterization and temperature depence of the 6H-SiC polytype and one on the piezoresistance of β-SiC (3C-SiC). In 1993, Shor et al. have extended this study on piezoresistive properties of β-SiC discussing the GF and the temperature coefficient of resistance (*TCR*) of this material for several doping levels. In 1997, Strass et al. investigated the influence of crystal quality on the piezoresistive effect in β-SiC. In 1998, Okojie et al. determined the longitudinal and transverse *GF* and the *TCR* of n- and p-type 6H-SiC.

In 2002, Toriyama & Sugiyama performed a theoretical analysis on the piezoresistivity of β-SiC based on electron transfer and the mobility shift mechanism and in 2004 a detailed experimental study on piezoresistive properties of single crystalline, polycrystalline, and nanocrystalline n-type 3C-SiC was reported by Eickhoff et al.
In parallel to these studies on characterization of piezoresistive properties of the SiC polytypes, some SiC sensors have been developed. In the ´90s, Okoije et al. developed 6H-SiC pressure sensors for high temperature applications and Ziermann et al. reported a piezoresistive pressure sensor with n-type β-SiC thin-film piezoresistors on Silicon-on-Insulators (SOI) substrate. In 2003, Atwell et al. simulated, fabricated and tested bulk micromachined 6H-SiC piezoresistive accelerometers.
The good performance exhibited by the sensors based on 6H-SiC bulk and on 3C-SiC film have motivated studies on the piezoresistive properties of amorphous SiC (a-SiC) films produced at low temperatures by techniques such as PECVD and magnetron sputtering (Fraga, 2010, 2011a; Fraga et al., 2011b, 2011c).
Table 1 presents the *GF* and *TCR* values of different SiC types and of some other materials commonly used in piezoresistive sensors. As can be observed, the p-type Si has the greater *GF* whereas the a-SiC film the smaller *TCR*.

Material	**Form**	**Dopant**	**Structure**	**GF** *	**TCR (ppm/°C)**
p-type Si	bulk	Boron	Crystalline	140	1082
n-type Si	bulk	Phosphorus	Crystalline	-133	1920
Ge	thin film	Boron	Amorphous	10	3100
Polysilicon	thin film	Boron	Polycristalline	34	100
a-SiC	thin film	Nitrogen	Amorphous	49	36
3C-SiC	thick film	Nitrogen	Crystalline	-31.8	400
6H-SiC	bulk	Nitrogen	Crystalline	15	-240

* GF measured at room temperature

Table 1. Comparison among the properties of some piezoresistive materials reported in literature (Fraga, 2011c; Shor, 1993; Okoije 1998a).

2.2 Physical description

The piezoresistive effect can also be defined as the tensor relationship between applied stress and change in resistivity (Johns, 2005):

$$\frac{\Delta\rho_{ij}}{\rho} = \pi_{ij}\sigma_{kl} \tag{3}$$

where ρ is the resistivity, π is the piezoresistive coefficient and σ is the mechanical stress. In the case of a material with cubic structure, the stress has six components σ_1, σ_2, and σ_3 (along the axes of the cube) and σ_4, σ_5, and σ_6 (the shear stresses) as shown in Figure 1.

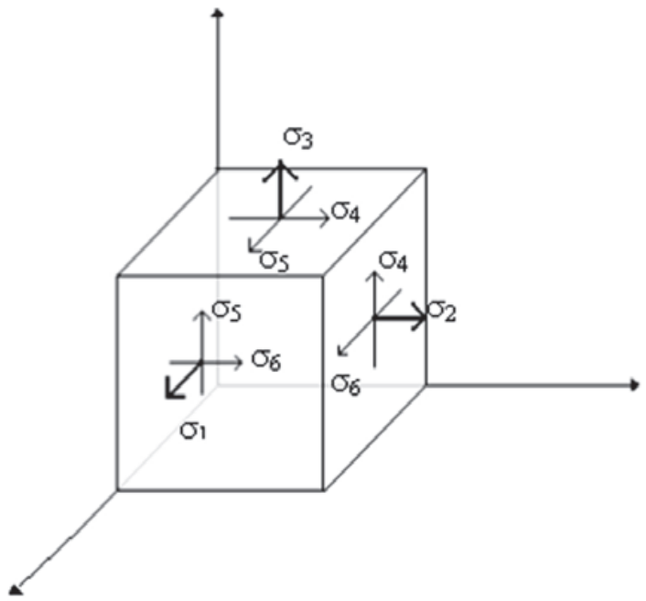

Fig. 1. Schematic illustration of the stress components.

The six stress components and six resistivity components result in a matrix with 36 piezoresistive coefficients. For the cubic crystal structure of materials such as silicon or β-SiC, the matrix simplifies to only three piezoresistive coefficients (π_{11}, π_{12}, and π_{44}) as shown in the following equation (Singh et al., 2002):

$$\begin{bmatrix} \frac{1}{\rho} \end{bmatrix} \begin{bmatrix} \Delta\rho_1 \\ \Delta\rho_2 \\ \Delta\rho_3 \\ \Delta\rho_4 \\ \Delta\rho_5 \\ \Delta\rho_6 \end{bmatrix} = \begin{bmatrix} \pi_{11} & \pi_{12} & \pi_{12} & 0 & 0 & 0 \\ \pi_{12} & \pi_{11} & \pi_{12} & 0 & 0 & 0 \\ \pi_{12} & \pi_{12} & \pi_{11} & 0 & 0 & 0 \\ 0 & 0 & 0 & \pi_{44} & 0 & 0 \\ 0 & 0 & 0 & 0 & \pi_{44} & 0 \\ 0 & 0 & 0 & 0 & 0 & \pi_{44} \end{bmatrix} \begin{bmatrix} \sigma_1 \\ \sigma_2 \\ \sigma_3 \\ \sigma_4 \\ \sigma_5 \\ \sigma_6 \end{bmatrix} \tag{4}$$

Although equation (4) models the piezoresistive effect in silicon in the direction of the crystal axes, customarily this effect is measured using only two coefficients: π_l that relates the resistance change due to stress in the longitudinal direction and π_t in the transverse direction. Therefore, the total resistivity change of a material can be simplified considering only changes under longitudinal and transverse stress components,

$$\frac{\Delta\rho}{\rho} = \pi_l\sigma_l + \pi_t\sigma_t \tag{5}$$

The piezoresistive effect can be better understood by the analysis of the behavior of a resistor when submitted to a mechanical stress. It is known that the electrical resistance of an unstressed resistor is given by,

$$R = \rho\frac{L}{A} \tag{6}$$

where L is the length and A the cross-sectional area of the resistor. When the resistor is subjected to a longitudinal stress, the resistivity, cross-sectional area and length will be changed as shown in the equation below:

$$\frac{\Delta R}{R} = \frac{\Delta \rho}{\rho} + \frac{\Delta L}{L} + \frac{\Delta A}{A} \tag{7}$$

This resistor that changes its resistivity with an applied stress is called piezoresistor. As can be observed in equation (7), a fractional resistance change, $\left(\frac{\Delta R}{R}\right)$, can be influenced by two factors: resistivity change $\left(\frac{\Delta \rho}{\rho}\right)$ and dimensions change $\left(\frac{\Delta L}{L}\right)$, $\left(\frac{\Delta A}{A}\right)$. The dominant factor depends on the material type. In your experiments, Smith observed that for silicon the change in resistivity gives a larger contribution to the resistance changes than the change in dimensions of the resistor (Smith, 1954).
Considering that the components associated with dimension change can be written as a function of the strain, we have:

$$\frac{\Delta L}{L} = \varepsilon_l \tag{8}$$

and

$$\frac{\Delta A}{A} = \frac{\Delta W}{W} + \frac{\Delta H}{H} = 2\varepsilon_t \tag{9}$$

In the above equations the fractional change in length is equal to the longitudinal strain whereas the change in area is the sum of change in width $\left(\frac{\Delta W}{W}\right)$ and height $\left(\frac{\Delta H}{H}\right)$. It is known that $\varepsilon_w = \varepsilon_H = \varepsilon_t$.
Considering also that the longitudinal and transverse strain are related through equation:

$$\varepsilon_t = \nu \varepsilon_l \tag{10}$$

where ν is the Poisson´s ratio of the material, thus the equation (7) can be simplified to

$$\frac{\Delta R}{R} = \frac{\Delta \rho}{\rho} + \varepsilon_l (1 + 2v) \tag{11}$$

Thus, the gauge factor can be related to resistivity, longitudinal strain and Poisson's ratio by the following equation (Allameh et al., 2006):

$$GF = \frac{1}{\varepsilon_l} \frac{\Delta \rho}{\rho} + (1 + 2v) \tag{12}$$

Another important parameter to evaluate the piezoresistive effect is the temperature, whose influence on strain measurement cannot be neglected. When the ambient temperature

changes, the electrical resistance of the resistor changes $\left(\frac{\Delta R}{R}\right)_{\Delta T}$. This influence is measured through temperature coefficient of resistance (*TCR*) and temperature coefficient of gauge factor (*TCGF*) that describe the parts per million change in resistance (or *GF*) for every one degree change in temperature. These coefficients can be determined by

$$TCR = \frac{1}{\Delta T}\frac{\Delta R}{R} = \frac{1}{\Delta T}\frac{R_T - R_0}{R_T} \tag{13}$$

$$TCGF = \frac{GF_T - GF_0}{GF_0}\frac{1}{\Delta T} \tag{14}$$

where ΔT is the change in temperature, R_0 and GF_0 are the electrical resistance and the gauge factor measured at room temperature or reference temperature (usually 25ºC), respectively; and R_T and GF_T are the electrical resistance and gauge factor measured at an operating temperature.

In a first analysis, the sensitivity of a piezoresistive sensor is evaluated in terms of *GF*, *TCR* and *TCGF*, i.e., a sensor with good performance should exhibit high *GF* and low *TCR*. For this, there is great interest by the piezoresistive characterization of materials with low *TCR*. In their study, Shor et al. reported that to reduce the effect of changing in temperature on the performance of a sensor the *TCR* should be positive and preferably constant, the *TCGF* negative and $|TCR| > |TCGF|$ (Shor et al., 1993).

In respect to the layout of a piezoresistive sensor, in general the most used configuration for the resistors is the Wheatstone bridge. In this configuration, four resistors are connected in loop as shown in Figure 2 and the output voltage is related to the input voltage according to the following equation:

$$\frac{V_{out}}{V_s} = \frac{V_A - V_B}{V_s} = \frac{R_3}{R_1 + R_3} - \frac{R_4}{R_2 + R_4} \tag{15}$$

where V_s is the supply voltage and V_{out} is the output voltage.

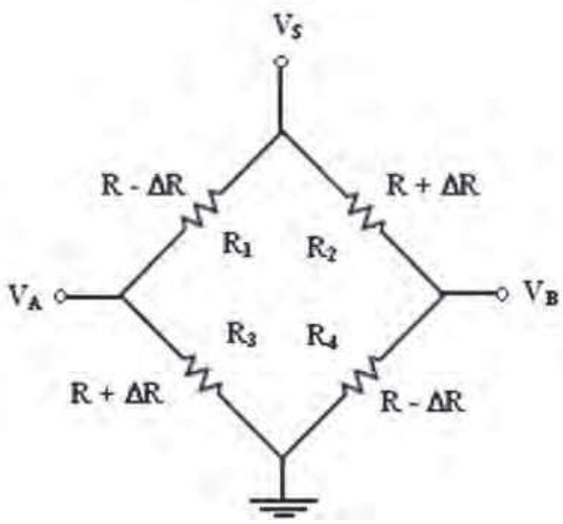

Fig. 2. Wheatstone bridge configuration.

When subjected to a mechanical stress, the electrical resistance of the resistors change leading to a variation of the output voltage, according to the following relationship

$$\frac{\Delta V_{out}}{V_s} = \frac{R_3 + \Delta R_3}{(R_1 + \Delta R_1) + (R_3 + \Delta R_3)} - \frac{R_4 + \Delta R_4}{(R_2 + \Delta R_2) + (R_4 + \Delta R_4)} \tag{16}$$

Whereas the four resistors have the same nominal resistance value (R_1=R_2=R_3=R_4) and that under mechanical stress the resistances R_2 and R_3 increases their values in +ΔR, the resistances R_1 and R_4 decreases their values in -ΔR. Therefore, the equation (16) can be simplified to

$$\frac{\Delta V_{out}}{V_s} = \frac{R + \Delta R}{2R} - \frac{(R - \Delta R)}{2R} = \frac{\Delta R}{R} \tag{17}$$

Given this, the sensitivity of a piezoresistive pressure sensor is determined by

$$S = \frac{\Delta R}{R}\frac{1}{\Delta P} = \frac{\Delta V_{out}}{V_s}\frac{1}{\Delta P} \tag{18}$$

where ΔP is change in pressure.
Whereas, for a piezoresistive accelerometer, the sensitivity is defined as the electrical output per unit of applied acceleration:

$$S = \frac{\Delta R}{R}\frac{1}{g} = \frac{\Delta V_{out}}{V_s}\frac{1}{g} \tag{19}$$

where g is the acceleration of gravity.

3. When and why to use SiC films in piezoresistive sensors?

As shown in the previous section, in recent years many researchers have been reported on the piezoresistive characterization of different SiC polytypes aiming the applicability of these materials in sensors. When comparing these studies, it is observed that for a same SiC polytype a dispersion of different values can be obtained for piezoresistive coefficient, *GF* and *TCR* (Okoije, 2002).
It is known that the SiC has about 200 polytypes with different physical properties. This is one of the difficulties in characterizing the piezoresistivity in SiC. Moreover, studies show that maximum value of *GF* for SiC at room temperature is between 30 at 49 while for the monocrystalline p-type Si is 140 (see Table 1). However, all studies published until now have demonstrated the potential of the 6H-SiC and 3C-SiC polytypes besides a-SiC for the development of piezoresistive sensors for high temperature application. Given this, it is important to evaluate when it is advantageous to use SiC in piezoresistive sensors and whether is better to use SiC in bulk or thin film form.
This analysis should begin with the following question: Why SiC?
Several studies show that the SiC has mechanical and chemical stability at high temperatures. Due to these characteristics the application of SiC sensors is always associated with harsh environments. In these environments, silicon has mechanical and chemical limitations. At temperature greater than 500ºC, silicon deforms plastically under small loads

(Pearson et al., 1957). In addition, the silicon does not support prolonged exposure to corrosive media. Another important factor that should be considered is that silicon pressure sensors using p-n junction piezoresistors have exhibited good performance at temperatures up to 175ºC and the SOI sensors at temperatures up to 500ºC.

Among the semiconductor materials with potential to substitute the silicon in harsh environments, SiC is the most appropriate candidate because its native oxide is SiO_2 which makes SiC directly compatible with the Si technology. This signifies that a sensor based on SiC can be developed following the same steps used in silicon sensors.

On the other hand, the chemical stability that have qualified SiC for harsh environments, makes it difficult to etch the bulk and to integrate any process step with already established Si based processes. Furthermore, the high cost of SiC wafer also difficult the development of "all of SiC" sensors. Faced with these difficulties the use of SiC thin films is quite attractive because the film can be grown on large-area Si substrates and by the ease of using conventional Si bulk micromachining techniques (Fraga et al., 2011a).

The second question is: When to use piezoresistive sensors based on SiC?

As already mentioned in the beginning of this section, at room temperature the monocrystalline silicon has greater *GF* than the SiC, i.e. sensors based on silicon operating on this condition has superior sensitivity. This fact shows that the use of SiC is only justified for specific applications in four main types of harsh environments, namely:

a. Mechanically aggressive that involve high loads as in oil and gas industry applications which require sensors to operate in pressure ranges up to 35,000 psi and at temperatures up to 200°C (Vandelli, 2008);
b. Thermally aggressive that involve high temperatures as in combustion control in gas turbine engines, where the operating temperatures are around 600°C (Vandelli, 2008) and in pressure monitoring during deep well drilling and combustion in aeronautical and automobile engines that require sensors to operate at temperatures ranging between 300 and 600ºC (Stanescu & Voican, 2007);
c. Chemically aggressive or corrosive environment as in biomedical and petrochemical applications where chemical attack by fluids is one of the modes of degradation of devices. The SiC sensors are a good choice for these applications because at room temperature, there is no known wet chemical that etches single-crystal SiC (George et al., 2006);
d. Aerospace environment where sensors should to maintain their functionality under high cumulative doses of radiation. Due to well known chemical inertness of the SiC, sensors based on this material have exhibited great potential for these applications.

4. Brief description of the main techniques to deposit SiC films

Several techniques for obtaining thin films and bulks of SiC have been developed. Some companies that manufacture crystalline silicon wafers also offer SiC bulk wafers up to 4 inches in diameter. However, SiC wafers have an average price fifteen times higher than Si wafers with the same dimensions (Hobgood et al., 2004; Camassel & Juillaguet, 2007). Besides the high cost, another problem of the use of SiC substrates is the difficult micromachining process and high density of defects (Wu et al., 2001). In this context, there is a crescent interest in deposition techniques of SiC films on Si or SOI (Silicon-On-Insulator) substrates. These films can be produced in crystalline and amorphous forms.

Crystalline SiC (c-SiC) thin films can be produced by techniques that use temperatures higher than 1000°C as chemical vapour deposition (CVD) (Chaudhuri et al., 2000), molecular beam epitaxy (MBE) (Fissel et al., 1995) and electron cyclotron resonance (ECR) (Mandracci et al., 2001). However, it is known that this high substrate temperature required for growing crystalline SiC onto Si substrate can degrade the quality of the SiC/Si interface leading to many defects in the grown films, which often prevents the film processing in conjunction with other microfabrication processes involved in a MEMS device fabrication. Conversely, there are attractive processes for the synthesis of thin films at low temperature as those based on plasma assisted techniques, such as plasma chemical vapour deposition (PECVD) and plasma sputtering, which operate at temperatures below 600°C (Rajagopalan et al., 2003; Lattemann et al., 2003). But SiC films obtained at low temperature processes are amorphous (a-SiC) or nano-crystallines (nc-SiC) and, thus, can exhibit properties somewhat different from those observed in crystalline films (Foti, 2001). Because of this, a process usually used to improve the crystallinity of the a-SiC films is the annealing (Rajab et al., 2006).

Among the techniques used to deposit SiC films, in this chapter only four of them will be described: CVD, PECVD, magnetron sputtering and co-sputtering. These techniques were chosen because have been used with success in the deposition of undoped and doped SiC films for MEMS sensors application. A common point among them is the ease to perform the "in situ" doping by the addition of dopant gas (N_2, PH_3 or B_2H_6) during the film deposition.

4.1 Chemical deposition processes: CVD and PECVD techniques

One of the most popular (laboratory) thin film deposition techniques nowadays are those based on chemical deposition processes such as chemical vapor deposition (CVD) and plasma enhanced chemical vapor deposition (PECVD) (Grill, 1994; Ohring, 2002; Bogaerts et al., 2002).

CVD or thermal CVD is the process of gas phase heating (by a hot filament, for example (Gracio et al., 2010)) in order for causing the decomposition of the gas, generating radical species that by diffusion can reach and be deposited on a suitably placed substrate. It differs from physical vapor deposition (PVD), which relies on material transfer from condensed-phase evaporant or sputter target sources (see section 4.2.). A reaction chamber is used for this process, into which the reactant gases are introduced to decompose and react with the substrate to form the film. Figure 3a illustrates a schematic of the reactor and its main components. Basically, a typical CVD system consists of the following parts: 1) sources and feed lines of gases; 2) mass flow controllers for metering the gas inlet; 3) a reaction chamber for decomposition of precursor gases; 4) a system for heating up the gas phase and wafer on which the film is to be deposited; and 5) temperature sensors.

Concerning the gas chemistry of CVD process for SiC film production, usually silane (SiH_4) and light hydrocarbons gases are used, such as propane or ethylene, diluted in hydrogen as a carrier gas (Chowdhury et al., 2011). Moreover, the main CVD reactor types used are atmospheric pressure CVD (APCVD) and low-pressure CVD (LPCVD).

As a modification to the CVD system, PECVD arose when plasma is used to perform the decomposition of the reactive gas source. By chemical reactions in the plasma (mainly electron impact ionization and dissociation), different kinds of ions and radicals are formed which diffuse toward the substrate where chemical surface reactions are promoted leading

to film growth. The major advantage compared to simple CVD is that PECVD can operate at much lower temperatures. Indeed, the electron temperature of 2–5 eV in PECVD is sufficient for dissociation, whereas in CVD the gas and surface reactions occur by thermal activation. Hence, some coatings, which are difficult to form by CVD due to melting problems, can be deposited more easily with PECVD (Bogaerts et al., 2002; Peng et al., 2011). Among the kinds of plasma sources that have been used for this application stand out the radiofrequency (rf) discharges (Bogaerts et al., 2002), pulsed discharges (Zhao et al., 2010) and microwave discharges (Gracio et al., 2010).

Basically, in PECVD the substrate is mounted on one of the electrodes in the same reactor where the species are created (see Figure 3b). Here, we focused the rf discharge because it is the configuration more used in research and industry. The rf PECVD reactor essentially consists of two electrodes of different areas, where the substrate is placed on the smaller electrode, to which the power is capacitively coupled. The rf power creates a plasma between the electrodes. Due to the higher mobility of the electrons than the ions, a sheath is created next to the electrodes containing an excess of ions. Hence, the sheath has a positive space charge, and the plasma creates a positive voltage with respect to the electrodes. The electrodes therefore acquire a dc self-bias equal to their peak rf voltage (self-bias electrode). The ratio of the dc self-bias voltages is inversely proportional to the ratio of the squared electrode areas, i.e., $V_1/V_2 = (A_1/A_2)^2$ (Lieberman & Lichtenberg, 2005).

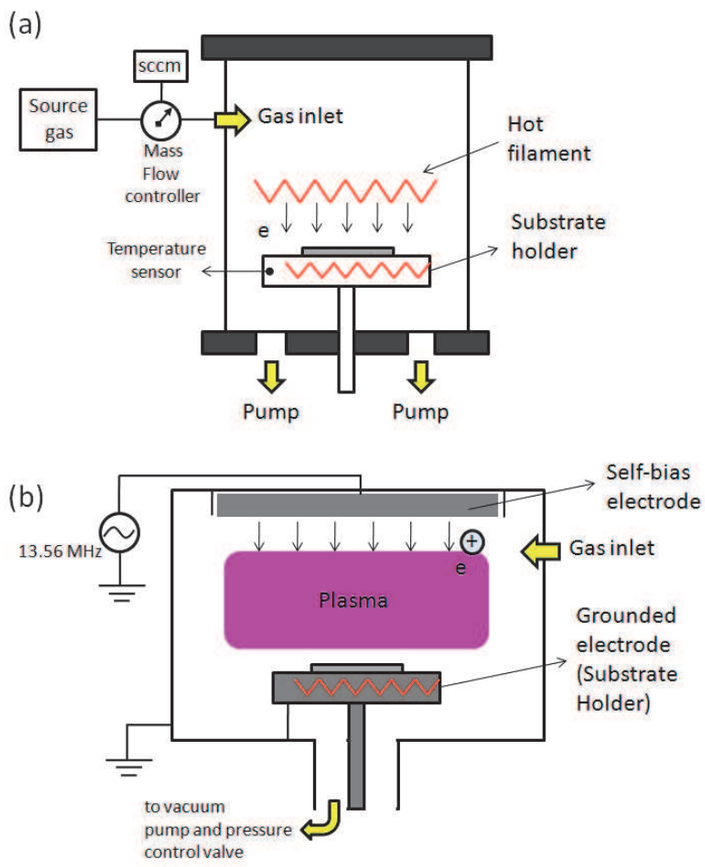

Fig. 3. Schematic diagram of CVD (a) and PECVD (b) systems.

Therefore, the smaller electrode acquires a larger bias voltage and becomes negative with respect to the larger electrode. The negative sheath voltage accelerates the positive ions towards the substrate which is mounted on this smaller electrode, allowing the substrate to become bombarded by energetic ions facilitating reactions with substrate surface.

In order to maximize the ion to neutral ratio of the plasma, the plasma must be operated at the lowest possible pressure. Nevertheless, the ions are only about 10 percent of the film-forming flux even at pressures as low as 50 mTorr. Lower pressures cannot be used as the plasma wills no longer strike. A second disadvantage of this source is the energy spread in the ion energy distribution, prohibiting a controlled deposition. This energy spread is due to inelastic collisions as the ions are accelerated towards the substrate. The effect of this energy spread is to lower the mean ion energy to about 0.4 of the sheath voltage. Still, another disadvantage of the rf PECVD source is that it is not possible to have independent control over the ion energy and the ion current, as they both vary with the rf power. On the other hand, PECVD allows the deposition of uniform films over large areas, and PECVD systems can be easily scaled up (Neyts, 2006).

The most used precursor gases to deposit SiC films by PECVD are SiH_4, as the silicon source, and methane (CH_4), as carbon source. Finally, Figure 4 illustrates the deposition mechanism of chemical vapor deposition technique (Grill, 1994). Basically the mechanism occurs by the following steps: (i) a predefined mix of reactant gases and diluents inert gases are introduced at a specified flow rate into the reaction chamber; (ii) a heat source is applied in order to dissociate the reactant gases; (iii) the resulting radical species diffuse to the substrate; (iv) the reactants get adsorbed on the surface of the substrate; (v) the reactants undergo chemical reactions with the substrate to form the film; and (vi) the gaseous by-products of the reactions are desorbed and evacuated from the reaction chamber.

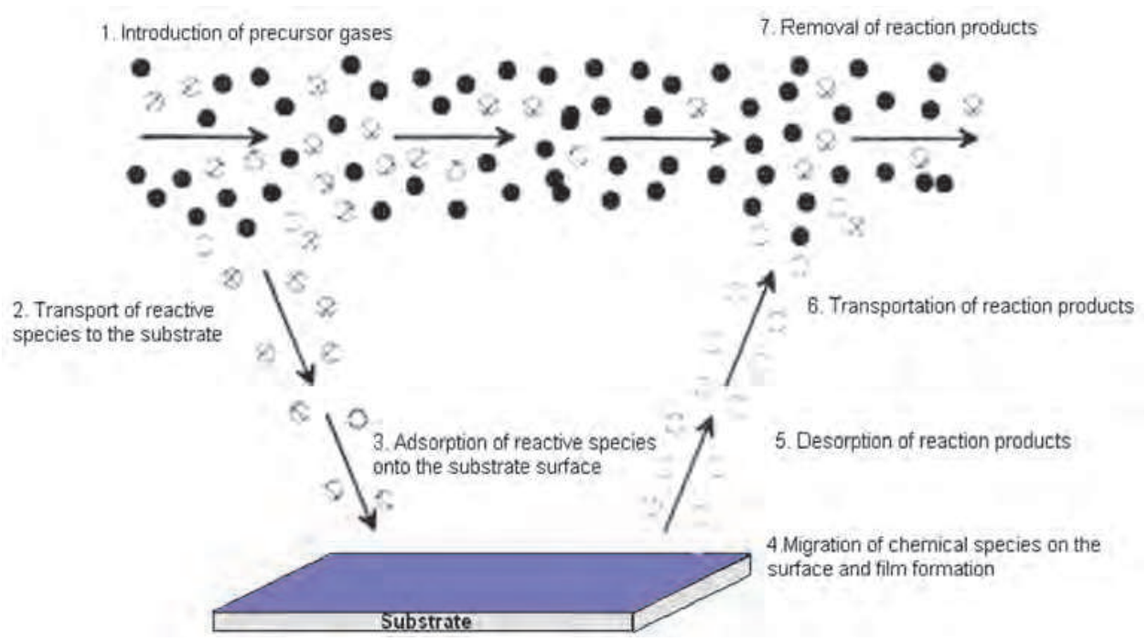

Fig. 4. Chemical vapor deposition mechanism. Adapted from (Doi, 2006).

4.2 Physical deposition processes: Magnetron sputtering and co-sputtering techniques

The physical deposition process comprise the physical sputtering and reactive sputtering techniques. Basically, these techniques differ when a neutral gas (physical sputtering) is added together with a reactive gas (reactive sputtering). In physical sputtering, ions (and atoms) from the plasma bombard the target, and release atoms (or molecules) of the target material. Argon ions at 500–1000 V are usually used. The sputtered atoms diffuse through the plasma and arrive at the substrate, where they can be deposited (Bogaerts et. al., 2002). In reactive sputtering, use is made of a molecular gas (for example, N_2 or O_2). Beside the positive ions from the plasma that sputter bombard the target, the dissociation products from the reactive gas will also react with the target. Hence, the film deposited at the substrate will be a combination of sputtered target material and the reactive gas (Bogaerts et al., 2002; Berg, 2005; Lieberman & Lichtenberg, 2005). The sputter deposition process is schematically presented in Figure 5.

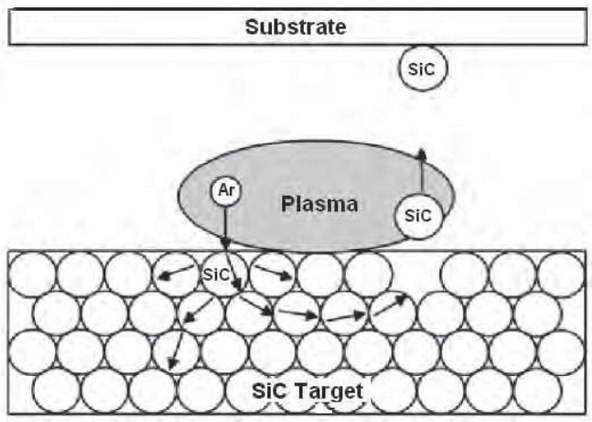

Fig. 5. Schematic of sputtering process.

Basically the steps of sputtering process are the following: (i) the neutral gas is ionized by a external power supply, producing a glow discharge or plasma; (ii) a source (the cathode, also called the target) is bombarded in high vacuum by gas ions due to the potential drop acceleration in the cathode sheath; (iii) atoms from the target are ejected by momentum transfer and diffuse through the vacuum chamber; (iv) atoms are deposited on the substrate to be coated and form a thin film.

Because sputter yields are of order unity for almost all target materials, a very wide variety of pure metals, alloys, and insulators can be deposited. Physical sputtering, especially of elemental targets, is a well understood process enabling sputtering systems for various applications to be relatively easily designed. Reasonable deposition rates with excellent film uniformity, good surface smoothness, and adhesion can be achieved over large areas (Lieberman & Lichtenberg, 2005).

Typically, the sputtering process can be accomplished using a planar configuration of electrodes and a dc power supply, where one electrode is biased negatively (cathode) and suffer the sputtering process. However, the sputtering yield is directly dependent on the gas pressure (best sputtering rates are in the range of mTorr) a fact that compromises the efficiency of planar geometry for this application: it is great for pressures above 100 mTorr. To solve this problem, it was developed the magnetron discharge where the plasma is magnetically enhanced by placing magnets behind the cathode target, i.e., a crossed electric and magnetic field configuration is

created. Figure 6 shows a schematic drawing of a conventional dc magnetron sputtering discharge. The trapping of the secondary electrons results in a higher probability of electron impact ionization and hence higher plasma density, increasing the sputtering flux and allowing operation at lower pressures, bellows 10 mTorr. Furthermore, the discharge voltage can be lowered into the range of 300-700 V. The main problem with the magnetron sputtering configuration is that the sputtering is confined to a small area of the target cathode governed by the magnetic field. The discharge appears in the form a high-density annulus of width w and radius R, as seen in Figure 6. Sputtering occurs in the corresponding track of the target. This area, known as the race track, is created by the uneven ion density.

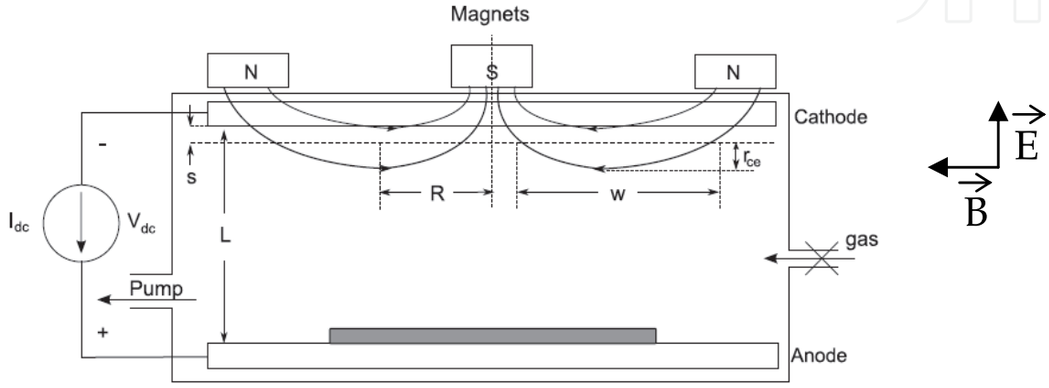

Fig. 6. Schematic drawing of a conventional dc magnetron sputtering discharge. Adapted from (Bogaerts et al., 2002).

Deposition of SiC films by the Magnetron Sputtering technique is performed generally using a SiC target in Ar atmosphere or a silicon target with precursor gases Ar plus CH_4 (Stamate et al., 2008). The dual magnetron (or co-sputtering) method also has been used to deposit SiC films. In this technique, the films are produced by co-sputtering of carbon and silicon targets (see Figure 7) with Ar as precursor gas (Kikuchi et al., 2002; Kerdiles et al., 2002). The co-sputtering technique offers as main advantage to obtaining of SiC films with different electrical, structural and mechanical properties by the variation of C/Si ratio in the film deposited (Kikuchi et al., 2002). Using this technique, it is possible to obtain a range of SiC film compositions by applied different power on each target (Medeiros et al., 2011).

5. Requirements of SiC films for piezoresistive sensors application

In order to develop piezoresistive sensors with high performance based on SiC films is necessary to optimize the properties of the SiC thin-film piezoresistors to maximize their sensitivity with the minimum temperature-dependent resistance variation (Luchinin & Korlyakov, 2009).

The first step for this optimization is the choice of the technique to deposit SiC films onto an insulator on Si substrates. Silicon dioxide (SiO_2) is the most used insulator material for this purpose, but some studies have showed silicon nitride (Si_3N_4) or aluminum nitride (AlN) as alternative materials. In general, good results have been achieved with the SiO_2, although this material has a coefficient of thermal expansion (*CTE*) significantly lower than the SiC, giving rise to thermal stresses at the SiC/SiO_2 interface. Many studies have shown CVD, PECVD and sputtering as appropriate techniques to deposit SiC films on SiO_2/Si (Zanola, 2004).

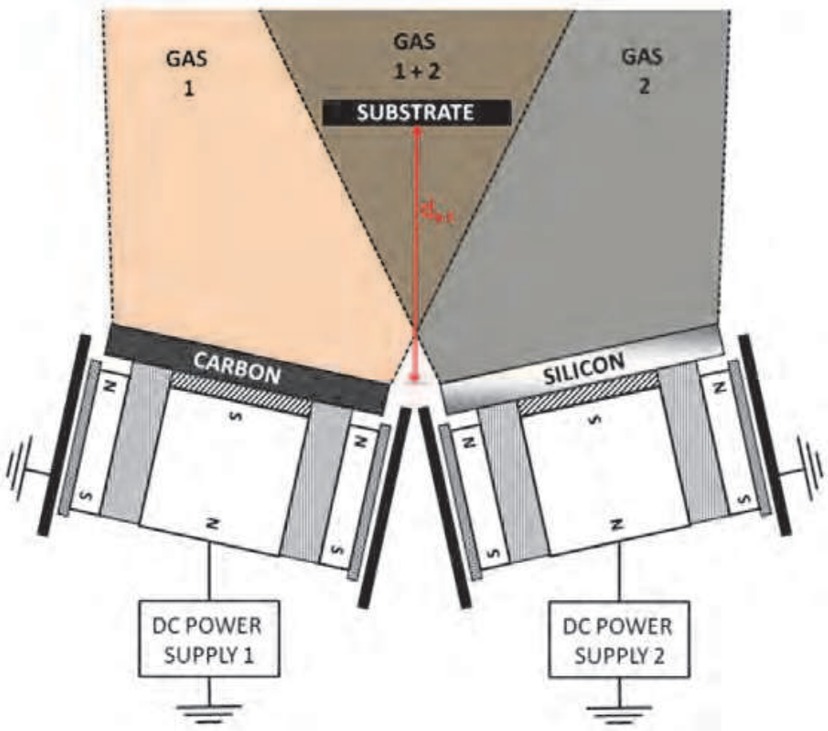

Fig. 7. Schematic diagram of magnetron co-sputtering deposition technique.

After the film deposition, the residual stress must be investigated. SiC films obtained by CVD have low residual stress due to high temperatures involved in this process. However, films obtained by PECVD and sputtering exhibit a significant tensile or compressive residual stress that is dependent on various deposition parameters. To reduce this stress post-deposition thermal annealing is usually performed (Zorman, 2006).

The following step is used to determine the chemical, physical and structural properties of the as-deposited SiC film. For piezoresistive sensor applications, it is fundamental the knowledge of the orientation, elastic modulus, doping concentration and resistivity of the film. After determining these properties, the piezoresistive characterization of the film is started. First, a test structure must be developed. Generally, this structure consists of a SiC thin-film piezoresistor fabricated by photolithography, lift-off and etching processes as illustrated in Figure 8.

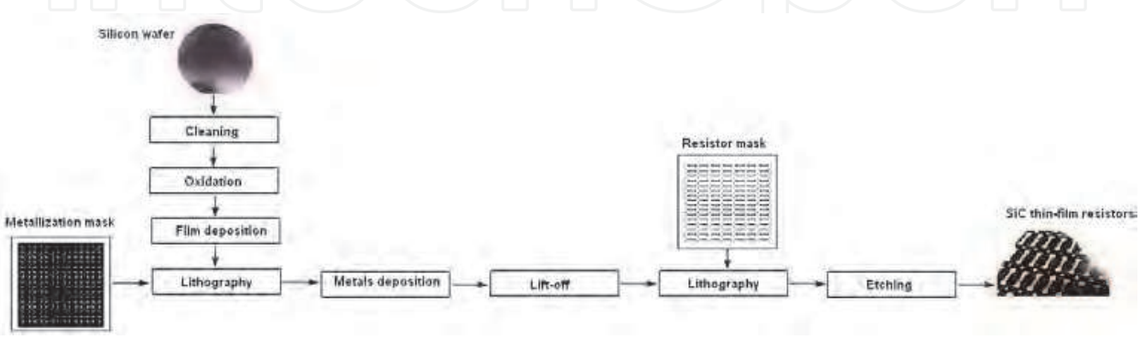

Fig. 8. Schematic flow diagram of the SiC thin-film resistor fabrication process.

The most used technique to determine the value of *GF* of a piezoresistor is the cantilever deflection method. In this method, the piezoresistor is glued near to the clamped end of a cantilever beam and on the free end of the beam different loads are applied. The value of *GF* is obtained by monitoring the resistance change when the resistor is subjected to different applied stress. Once determined the *GF*, the *TCR* and the *TCGF* are determined to evaluate the influence of the temperature (see details on topic 2).
Table 2 summarizes the main requirements that SiC film should present to be successfully used in the development of piezoresistive sensors. As can be seen, the resistivity of the SiC thin film should be low (preferably of the order of mΩ.cm) because its thickness in general less than 1.0 μm. As the depth of the SiC thin-film piezoresistor is equals the thickness film, it is necessary a low resistivity film to form low electrical resistance piezoresistors.

Electrical and Mechanical Characteristics	**Requirement**
Elastic modulus	The greater
Residual stress	The lower
Resistivity	The lower
GF	The greater
TCR	The lower
TCGF	The lower

Table 2. Main requirements of SiC films for piezoresistive sensor applications.

6. Examples of piezoresistive sensors based on SiC films

Among the many silicon-based microsensors, piezoresistive pressure sensors are one of the widely used products of microelectromechanical system (MEMS) technology. This type of sensor has dominated the market in recent decades due to characteristics such as high sensitivity, high linearity, and an easy-to-retrieve signal through bridge circuit. The main applications of Si-based piezoresistive pressure sensors are in the biomedical, industrial and automotive fields. However, these sensors have a drawback that is the influence of the temperature on their performance. For some applications, this temperature effect can be compensated by an external circuit, which adds substantial cost to the sensor.
Given this, many studies have been performed aiming to reduce the temperature effects on the performance of the sensor through the use of piezoresistive sensing elements formed by wide bandgap semiconductor thin film as the SiC. The goal is to develop sensors as small as possible and enable to operate at high temperatures. For this, besides making the piezoresistors based on material with suitable properties for high temperature applications should also be used stable electrical contacts with excellent environmental stability. It is known that the metallization type also influences the performance of the devices at harsh environments. Studies show that for SiC sensors the best high-temperature contacts are metal as Au, Ni, Ti and W and binary compounds such as $TiSi_2$ and $WiSi_2$ (Cocuzza, 2003).
A typical SiC thin-film based piezoresistive pressure sensor consists of SiC thin-film piezoresistors, configured in Wheatstone bridge, on a diaphragm. The monocrystalline silicon is the material most used to form the diaphragm due its mechanical properties which make it an excellent material for elastic structural members of a sensor. In addition, the Si diaphragms can be easily fabricated by KOH anisotropic etching from the backside of a (100) silicon wafer using

the SiO_2 or Si_3N_4 film as etch mask. It is also necessary to grow SiO_2 or Si_3N_4 on the front side of the wafer to perform the electrical insulation of the SiC thin-film piezoresistors from the substrate. Generally, the SiC thin-film piezoresistors are produced by RIE (reactive ion etching). Figure 9 illustrates two piezoresistive pressure sensors based on SiC films: one with six PECVD a-SiC thin-film piezoresistors, configured in Wheatstone bridge, on a SiO_2/Si square diaphragm with Ti/Au metallization (Fraga et al., 2011b) and the other with phosphorus-doped APCVD polycrystalline 3C-SiC piezoresistors on Si_3N_4/3C-SiC diaphragm with Ni metallization (Wu et al., 2006).

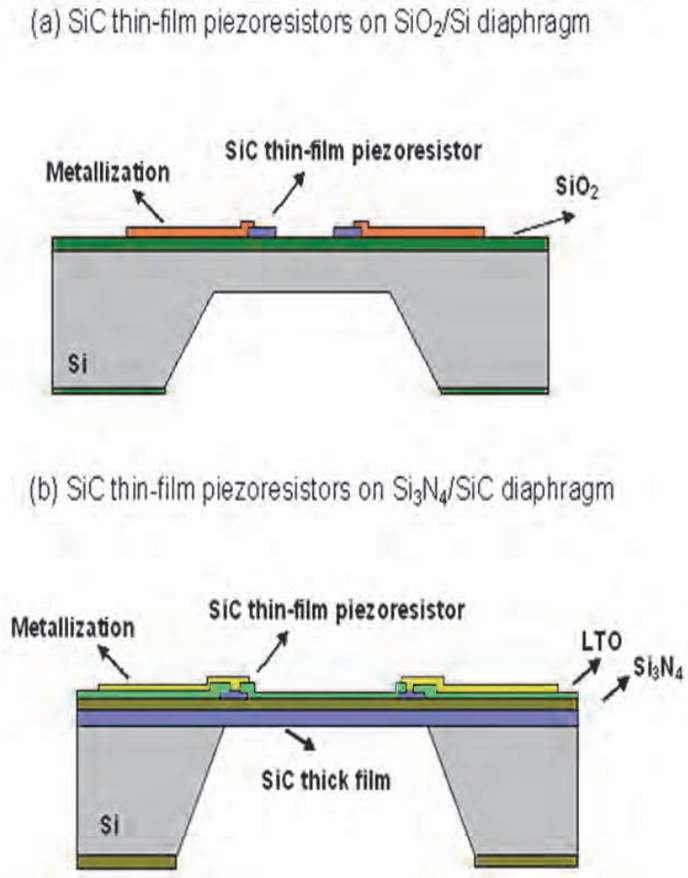

Fig. 9. Schematic illustration of piezoresistive pressure sensors based on SiC films.

Another sensor type that has been developed based on SiC is the accelerometer. However, for now, the studies are still focused on piezoresistive accelerometers based on 6H-SiC bulk substrate (Atwell et al., 2003) or on SiC thin-film capacitive accelerometers (Rajaraman et al., 2011).

This occurs because the capacitive accelerometer is usually more sensitive than piezoresistive one and furthermore can be used in a wide range of temperature. On the other hand, the capacitive accelerometers have elevated cost and necessity of signal conditioning circuit (Koberstein, 2005). The motivation to develop piezoresistive accelerometers on 6H-SiC bulk is the possibility of obtaining superior performance at high temperature in comparison with capacitive accelerometer.

As mentioned earlier, the cost of the 6H-SiC is also elevated which has stimulated the researches on SiC thin-film piezoresistive accelerometer. The simplest model for this accelerometer is illustrated in Figure 10. This accelerometer consists of a SiC thin-film piezoresistor (or four piezoresistors configured in Wheatstone bridge) on a silicon cantilever beam which has a rigid silicon proof mass attached at its free end. The basic principle of this type of sensor is that the acceleration moves the proof mass so deflecting the cantilever which works as a spring. The mass shift produces a variation of the internal stress of the spring that can be sensed by the piezoresistor. The value of the acceleration can be inferred by the measurement of the magnitude of the stress. The main problem of this accelerometer is that all its structure is built on silicon which can limit the performance at harsh environments.

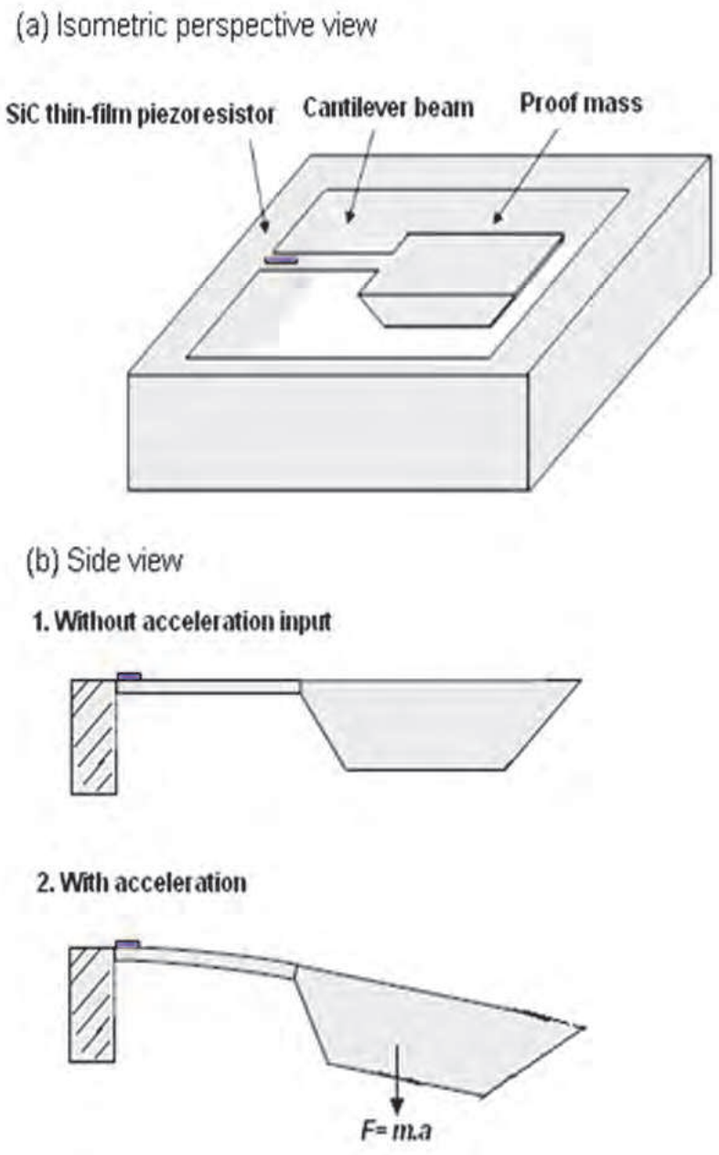

Fig. 10. Schematic illustration of a SiC thin-film based piezoresistive accelerometer.

7. Summary

It is notable that in recent years significant advances have been made in the SiC thin film technology for piezoresistive sensors application. These advances include improvement of deposition techniques to optimize the electrical, mechanical and piezoresistive properties of crystalline and amorphous SiC films which have enabled the development of sensors appropriate for harsh environments with costs lower than those based on SiC bulk.
This chapter reviewed the concepts of piezoresistivity, presented a brief survey on the studies of piezoresistive properties of SiC films, described the main techniques that are being used to deposit SiC films for MEMS sensor applications, discussed when and why to use SiC and what are the requirements that SiC films must attain to be applied successfully in piezoresistive sensors. Futhermore, it was shown examples of SiC film based pressure sensors and accelerometers.

8. Acknowledgments

The authors acknowledge the financial support of Brazilian agencies: program PNPD-CAPES (process number 02765/09-8), CNPq (process number 152912/2010-0) and AEB. We also would like to thank the institutions that have provided their infrastructure for the experiments: Plasma and Processes Laboratory of the Technological Institute of Aeronautics, Microfabrication Laboratory of the Brazilian Synchrotron Light Laboratory (LMF-LNLS), Institute for Advanced Studies (IEAv), Center of Semiconductor Components (CCS-UNICAMP), Faculty of Technology of São Paulo (FATEC-SP) and Associate Laboratory of Sensors (LAS-INPE).

9. References

Allameh, S. M.; Soboyejo, W.O.; Srivatsan, T.S. (2006) *Silicon-Based Microelectromechanical Systems (Si-MEMS)*, In: *Advanced Structural Materials: Properties, Design Optimization, and Applications*, pp.63-94.

Atwell, A.R.; Okojie, R.S., Kornegay, K.T.; Roberson, S.L.; Beliveau, A. (2003) *Sensors and Actuators A: Physical*, Vol.104, pp.11-18.

Berg, S.; Nyberg, T. (2005) *Thin Solid Films*, Vol.476, pp.215-230.

Bogaerts A.; Neyts E.; Gijbels R.; Mullen J. (2003) *Spectrochimica* Acta Part B, Vol.57, pp.609–658.

Camassel, J.; Juillaguet, S. (2007) J. *Phys. D: Appl. Phys*., Vol.40, pp.6264-6277.

Chaudhuri, J.; Ignatiev, K.; Edgar, J.H.; Xie, Z.Y.; Gao, Y.; Rek, Z. (2000) *Mater. Sci. Eng. B*, Vol.76, pp.217-224.

Chowdhury, I.; Chandrasekhar, M.V.S.; Klein, P.B.; Caldwell, J.D.; Sudarshan, T. (2011) *Journal of Crystal Growth*, Vol.316, pp.60-66.

Cimalla, V.; Pezoldt, J.; Ambacher, O. (2007) J. *Phys. D: Appl. Phys*., Vol.40, pp.6386-6434.

Cocuzza, M. (2003) *Development of silicon and silicon carbide-based micro-electromechanical systems*, PhD thesis, Polytechnic of Turin.

Doi, I. (2006) *Técnicas de deposição: CVD, notas de aula da disciplina IE726 – Processos de Filmes Finos*, Universidade Estadual de Campinas.

Eickhoff, M.; Möller, M.; Kroetz, G.; Stutzmann, M. (2004) *J. Appl. Phys*., Vol.96, pp. 2872-2877.

Fissel, A.; Kaiser, U.; Ducke, E.; Schroter, B.; Richter, W. (1995) *J. Cryst. Growth*, Vol.154, pp.72-80.

Foti, G. (2001) *Applied Surface Science* Vol.184, pp.20–26.
Fraga, M.A. (2009) *Desenvolvimento de sensores piezoresistivos de SiC visando aplicação em sistemas aeroespaciais*, PhD thesis, Instituto Tecnológico de Aeronáutica.
Fraga, M.A.; Furlan H.; Massi, M.; Oliveira I.C. (2010a) *Microsyst Technol*., Vol. 16, pp.925-930.
Fraga, M.A (2011a) *Materials Science Forum*, Vol. 679-680, pp.217-220.
Fraga, M.A.; Furlan, H.; Massi, M.; Oliveira, I.C.; Mateus, C.F.R.; Rasia, L.A. ; (2011b) *Microsyst. Technol*., In press.
Fraga, M.A.; Furlan H.; Pessoa, R.S. (2011c) *Comparison among performance of strain sensors based on different semiconductor thin films, Proceedings of the SPIE Microtechnologies - Smart Sensors, Actuators and MEMS Conference*, Prague, April 2011.
George T.; Son K.A.; Powers R.A.; Del Castillo L.Y.; Okojie R. (2006) *Harsh environment microtechnologies for NASA and terrestrial applications, Proceedings of IEEE sensors*, Irvine, November 2005.
Gracio, J. J.; Fan, Q. H.; Madaleno, J. C. (2010) *J. Phys. D: Appl. Phys.*, Vol.43, 374017 (22pp).
Grill, A. (1994) *Cold Plasmas in Materials Fabrication: From Fundamentals to Applications*, IEEE Press, 257p.
Guk, G. N.; Usol´tseva, N.Y.; Shadrin, V.S.; Mundus-Tabakaev, A.F. (1974a) *Sov. Phys. Solid State,* Vol.8, pp. 406-407 as cited in (Okoije, 2002).
Guk, G.N.; Lyubimskii, V.M.; Gofman, E.P.; Zinovév, V.B; Chalyi, E.A. (1974b) *Sov. Phys. Solid State,* pp.104-105.
Guk, G. N. ; Usol´tseva, N.Y. ; Shadrin, V.S. ;Prokop´eva, N.P (1976) *Sov. Phys. Solid State,* Vol. 10, pp.83-84 as cited in (Shor et al., 1993).
Hobgood, H. McD.; Brady, M. F.; Calus, M. R.; Jenny, J. R.; Leonard, R. T.; Malta, D. P.; Müller, S. G.; Powell, A. R.; Tsvetkov, V. F.; Glass, R. C.; Carter, C. H. (2004) *Mater. Sci. Forum*, Vol.457-460, pp.3-8.
Johns, G.K. (2005) *Journal of Applied Engineering Mathematics*, Vol. 2, pp. 1-5.
Kerdiles, S.; Rizk, R.; Gourbilleau, F.; Perez-Rodriguez, A.; Garrido, B.; Gonzalez-Varona, O.; Morante, J.R. (2002) *Materials Science and Engineering B*, Vol.69–70, pp.530–535.
Kikuchi, N; Kusano, E.; Tanaka, T.; Kinbara, A.; Nanto, H. (2002) *Surface and Coatings Technology*, Vol.149, pp.76–81.
Koberstein, L. (2005) *Modelagem de um acelerômetro de estado sólido, Master dissertation in Electrical Engineering*, University of São Paulo.
Kulikovsky V. ; Vorlíček, V.; Boháč, P.; Stranyánek, M.; Čtvrtlík, R. ; Kurdyumov, A. ; Jastrabik, L. (2008) *Surface & Coatings Technology,* Vol.202, pp.1738–1745.
Lattemann, M.; Nold, E.; Ulrich, S.; Leiste, H.; Holleck, H. (2003) *Surface and Coatings Technology*, Vol.174-175, pp.365-369.
Lieberman, M.A.; Lichtenberg, A.J. (2005) *Principles of Plasma Discharges and Materials Processing, 2nd edn*, New York: Wiley.
Luchinin, V.V.; Korlyakov, A.V. (2009), *Materials and elements of constructions for extreme micro- and nanoengineering, Proceedings of the EUROCON,* pp.1242-1245.
Mandracci, P.; Chiodoni, A.; Cicero, G.; Ferrero, S.; Giorgis, F.; Pirri, C.F.; Barucca, G.; Musumeci, P.; Reitano, R. (2001) *Applied Surface Science* Vol.184, pp.43-49.
Medeiros, H. S.; Pessoa, R.S.; Sagás, J.C.; Santos, L.V.; Fraga, M.A.; Maciel, H.S.; Sobrinho, A. S. S.; Massi, M. (2010) *Effect of Concentration of Carbon and Silicon in the SiC Thin Film Deposition by Dual Magnetron Sputtering System*, In : IX SBPMat, Ouro Preto-MG, Brazil.
Morin, F. J.; Geballe, T. H.; Herring, C. (1956) *Physical Review*, Vol.10, No.2, pp.525-539.
Neyts, E. (2006) *Mathematical Simulation of the Deposition of Diamond-like carbon (DLC) Films*, PhD thesis, Universiteit Antwerpen.

Okojie, R.S.; Ned, A.A.; Kurtz, A.D.; Carr, W.N. (1996) α(6H)-*SiC pressure sensors for high temperature applications*, Micro Electro Mechanical Systems (MEMS '96) Proceedings, pp.146-149.

Okojie, R.S.; Ned, A.A.; Kurtz, A.D.; Carr, W.N. (1998a) *IEEE Trans. Elec. Dev.*, Vol. 45, pp.785-790.

Okojie, R.S.; Ned, A.A.; Kurtz, A.D. (1998b) *Sensors and Actuators A: Physical*, Vol.66, pp.200-204.

Okojie, R.S. (2002) *Fabrication and characterization of single-crystal silicon carbide MEMS.* In: *MEMS Handbook*, Mohamed Gad-el-Hak, pp.20.1-20.31, CRC Press.

Ohring, M. (2002) *Material Science of Thin Films: Deposition & Structure*, San Diego, CA : Academic Press, 2º edition, 794 p.

Pearson, G.L.; Read Jr., W.T.; Feldman, W.L. (1957) *Acta Mettalurgica*, Vol. 5, pp.181-191.

Peng, X.; Matthews, A.; Xue, S. (2011) J. *Mater. Sci.*, Vol.46, pp.1–37.

Rajab, S.M.; Oliveira, I.C.; Massi, M.; Maciel, H.S.; dos Santos Filho, S.G.; Mansano, R.D. (2006) *Thin Solid Films*, Vol.515, pp.170-175.

Rajagopalan, T.; Wang, X.; Lahlouh, B.; Ramkumar, C.; Dutta, P.; Gangopadhyay, S. (2003) *Journal of Applied Physics*, Vol.94(8), pp.5252-5260.

Rajaraman, V.; Pakula, L.S.; Yang, H.; French, P.J.; P. M. Sarro (2011) *Int J Adv Eng Sci Appl Math*, Vol. 2, pp. 28-34

Rapatskaya, I.V.; Rudashevskii, G.E.; Kasaganova, M.G.; Islitsin, M.I.; Reifman, M.B.; E.F. Fedotova, E.F. (1968) *Sov. Phys. Solid State*, Vol. 9, pp. 2833-2835 as cited in Okoije, 2002.

Singh, R.; Ngo, L.L.; Seng H.S.; Mok, F.N.C. (2002) *A Silicon piezoresistive pressure sensor, Proceedings of the First IEEE International Workshop on Electronic Design, Test and Applications*, pp.181-184.

Shor, J.S.; Goldstein, D.; Kurtz, A.D. (1993) *IEEE Trans. Elec. Dev.*, Vol. 40, pp.1093-1099.

Smith, C.S. (1954) *Physics Review,* Vol. 94, pp. 42–49.

Stamate, M.D.; Lazar, I.; Lazar, G. (2008) *Journal of Non-Crystalline Solids,* Vol.354, pp.61–64.

Stanescu, C.D.; Voican, C. (2007) *Accelerated Stress Testing of SiC Pressure Tranduce, In: Proceedings of Fascicle of Management and Technological Engineering,* Vol. VI, pp.779-784.

Strass, J.; Eickhoff, M.; Kroetz, G. (1997) *The influence of crystal quality on the piezoresistive effect of β-SiC between RT and 450°C measured by using microstructures*, In: *International Conference on Solid State Sensors and Actuators,* Vol. 2, pp.1439-1442.

Toriyama, T.; Sugiyama S. (2002) *Appl. Phys. Lett.*, Vol. 81, pp.2797-2799.

Vandelli, N. (2008) *SiC MEMS Pressure Sensors for Harsh Environment Applications, MicroNano* News, pp.10-12.

Window, A.L. (1992) *Strain Gauge Technology*, Springer, London.

Wright, N. G.; Horsfall, A. B. (2007) *J. Phys. D: Appl. Phys.*, Vol. 40, pp.6345-6354.

Wu, C.H.; Stefanescu, H.; Zorman, C. A.; Mehregany, M. (2001) *Fabrication and Testing of Single Crystalline 3C-SiC piezoresistive Pressure Sensors*, In: *Eurosensors XV.*

Wu C.H.; Zorman C.A..; Mehregany M. (2006) *IEEE Sensors Journal*, Vol.6, pp. 316-324.

Zanola,P.; Bontempi, E.; Ricciardi, C.; Barucca, G.; Depero, L.E. (2004) *Materials Science and Engineering B*, Vol.114-115, pp. 279-283.

Zhao, D.; Mourey, D.A.; Jackson, T.N. (2010) *Journal of Electronic Materials*, Vol. 39, No. 5, pp. 554-558.

Ziermann, R.; von Berg, J.; Reichert, W.; Obermeier, E.; Eickhoff, M.; Krotz, G. (1997) *A high temperature pressure sensor with β-SiC piezoresistors on SOI substrates, International Conference on Solid State Sensors and Actuators*,Chicago, June 1997.

Zorman, C.A.; Fu, X.; Mehregany M. (2006) *Deposition techniques for SiC MEMS In: Silicon Carbide Micro Electromechanical Systems*, pp. 18-45.

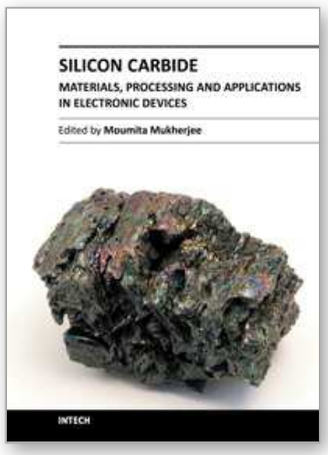

Silicon Carbide - Materials, Processing and Applications in Electronic Devices

Edited by Dr. Moumita Mukherjee

ISBN 978-953-307-968-4
Hard cover, 546 pages
Publisher InTech
Published online 10, October, 2011
Published in print edition October, 2011

Silicon Carbide (SiC) and its polytypes, used primarily for grinding and high temperature ceramics, have been a part of human civilization for a long time. The inherent ability of SiC devices to operate with higher efficiency and lower environmental footprint than silicon-based devices at high temperatures and under high voltages pushes SiC on the verge of becoming the material of choice for high power electronics and optoelectronics. What is more important, SiC is emerging to become a template for graphene fabrication, and a material for the next generation of sub-32nm semiconductor devices. It is thus increasingly clear that SiC electronic systems will dominate the new energy and transport technologies of the 21st century. In 21 chapters of the book, special emphasis has been placed on the â€œmaterialsâ€ aspects and developments thereof. To that end, about 70% of the book addresses the theory, crystal growth, defects, surface and interface properties, characterization, and processing issues pertaining to SiC. The remaining 30% of the book covers the electronic device aspects of this material. Overall, this book will be valuable as a reference for SiC researchers for a few years to come. This book prestigiously covers our current understanding of SiC as a semiconductor material in electronics. The primary target for the book includes students, researchers, material and chemical engineers, semiconductor manufacturers and professionals who are interested in silicon carbide and its continuing progression.

INTECH
open science | open minds

InTech Europe
University Campus STeP Ri
Slavka Krautzeka 83/A
51000 Rijeka, Croatia

InTech China
Unit 405, Office Block, Hotel Equatorial Shanghai
No.65, Yan An Road (West), Shanghai, 200040, China
中国上海市延安西路65号上海国际贵都大饭店办公楼405单元

Phone: +385 (51) 770 447
Fax: +385 (51) 686 166
www.intechopen.com

Phone: +86-21-62489820
Fax: +86-21-62489821

IntechOpen

IntechOpen